PHYSICAL REVIEW B VOLUME 44, NUMBER 14 1 OCTOBER 1991-II

Complete solution of the antiferromagnetic Heisenberg rings with $N = 12-16$ sites

K. Fabricius, U. Löw, K.-H. Mütter, and P. Ueberholz
Physics Department, University of Wuppertal, D-5600 Wuppertal, Germany

(Received 21 January 1991; revised manuscript received 17 April 1991)

We present results of a complete and exact diagonalization of the antiferromagnetic Heisenberg Hamiltonian for rings with $N = 12$, 13, 14, 15, or 16 sites.

I. INTRODUCTION

There has been a considerable effort over more than 60 years to achieve a better understanding of the spin-$\frac{1}{2}$ quantum Heisenberg system. Some analytical results are known for one-dimensional rings with periodic boundary conditions: (1) Bethe's ansatz[1] allows for an exact computation of some quantities in the thermodynamical limit, e.g., the ground-state energy. However, there are also quantities of physical interest which are not easily accessible via the Bethe ansatz, e.g., wave functions and spin-spin correlation correlation functions. (2) There exist higher conservation laws.[2] The associated quantum numbers can be used for a complete characterization of the energy eigenstates and their degeneracies.[3]

The antiferromagnetic Heisenberg (AFH) model with a limited number N of sites was studied numerically. The ground state has been computed by Oitmaa and Betts[4] on lattices up to 16 sites. Using a modified Lanczos algorithm, the authors in Ref. 5 were able to enlarge the size of the lattice to 24 sites. A complete diagonalization of the AFH Hamiltonian for rings with $N = 2-11$ was performed by Bonner and Fisher.[6] They were able to compute exactly the thermodynamical and magnetic properties of the model. These results, obtained on rather small systems, yield a useful check for "less exact" algorithms like Monte Carlo,[7] which can be performed on much larger systems. It is the purpose of this paper to present the results of a complete and exact diagonalization of the AFH Hamiltonian with $N = 12-16$ sites. The outline of the paper is as follows. In Sec. II we discuss the quantum numbers which characterize the energy eigenstates and show the distribution of the energy eigenvalues and their degeneracies. In Secs. III and IV, the thermodynamical and magnetic properties of the AFH model are presented and compared with the previous results of Bonner and Fisher.[6] Spin-correlation functions and the temperature dependence of the correlation length are studied in Sec. V. From a finite-size scaling analysis we conclude that the correlation length $\xi(T, N \to \infty)$ diverges with a critical exponent close to one as we approach zero temperature ($T \to 0$). In Sec. VI, we present results on thermal averages of an operator corresponding to a "higher" conservation law in the one-dimensional quantum Heisenberg model. Finally, in Sec. VII, we discuss the surprising behavior of the thermal average of the modulus of the momentum: In the thermodynamical limit it seems to be $\pi/2$, independent of the temperature.

II. ENERGY EIGENVALUES: DISTRIBUTIONS AND DEGENERACIES

The isotropic AFH Hamiltonian for periodic rings with N sites is defined by

$$H = \frac{1}{2} \sum_{x=1}^{N} \boldsymbol{\sigma}(x) \cdot \boldsymbol{\sigma}(x+1) , \tag{2.1}$$

where

$$\boldsymbol{\sigma} = (\sigma_1, \sigma_2, \sigma_3)$$

is the vector of Pauli matrices. The obvious symmetries of H are the following.

(1) Translation invariance, leading to momentum conservation,

$$[H, P] = 0 . \tag{2.2}$$

(2) Reflection invariance

$$[H, R] = 0 . \tag{2.3}$$

The reflection operator R transforms states with momentum p into those with momentum $-p$. Therefore, it anticommutes with the momentum operator

$$\{R, P\} = 0 . \tag{2.4}$$

(3) Rotation invariance, which implies the conservation of total spin:

$$\mathbf{S} = \sum_x \mathbf{S}(x) , \quad [H, \mathbf{S}] = 0 . \tag{2.5}$$

The total spin operator is translation and reflection invariant:

$$[\mathbf{S}, P] = 0, \quad [\mathbf{S}, R] = 0 . \tag{2.6}$$

In addition, there is an infinite set of "higher" conservation laws F_n. For the classification of energy eigenstates, the most important one is

$$\begin{gathered} F_3 = i \sum_x \varepsilon(x, x+1, x+2) , \\ [H, F_3] = [P, F_3] = [\mathbf{S}, F_3] = 0 \end{gathered} \tag{2.7}$$

with

$$\varepsilon(x_1, x_2, x_3) = \varepsilon_{abc} S_a(x_1) S_b(x_2) S_c(x_3) . \tag{2.8}$$

F_3 commutes with H, $\mathbf{S}$, P, but anticommutes with R:

$$\{F_3,R\}=0 \ . \tag{2.9}$$

We classify the eigenstates

$$|E,s,s_3,p,\lambda\rangle \tag{2.10}$$

by the eigenvalues of H, S, S_3, P, F_3. Due to the anticommutation rules (2.4) and (2.9), the states

$$R|E,s,s_3,p,\lambda\rangle \tag{2.11}$$

are eigenstates of P and F_3 with eigenvalues $(-p,-\lambda)$. On the other hand, H is symmetric under R. Therefore, the eigenstates (2.10) and (2.11) have degenerate energy eigenvalues. In other words, there is at least a twofold degeneracy of all eigenstates with quantum numbers (p,λ) and $(-p,-\lambda)$. Nondegenerate energy eigenstates must have quantum numbers $(p=0,\pi;\ \lambda=0)$. In particular, the nondegenerate ground state is found in the sector characterized by the quantum numbers

$$\begin{aligned} &s=0,\ p=0,\ \lambda=0 \quad \text{for } N=4,8,\dots,\\ &s=0,\ p=\pi,\ \lambda=0 \quad \text{for } N=6,10,\dots\ . \end{aligned} \tag{2.12}$$

The first excited state has quantum numbers

$$\begin{aligned} &s=1,\ p=\pi\ ,\lambda=0 \quad \text{for } N=4,8,\dots,\\ &s=1,\ p=0,\ \lambda=0 \text{ for } N=6,10,\dots\ . \end{aligned} \tag{2.13}$$

The situation looks quite different for rings with an odd number of sites where the ground state and the first excited state have spin $\frac{1}{2}$ and $\frac{3}{2}$, respectively. The momenta of the ground state and the first excited state are listed in Table I.

From Table I we read off the following rules for the momenta in the ground state and in the first excited state:

$$\begin{aligned} &|p_0|=\pi/2(1+1/N),\ |p_1|=\pi/2(1-3/N)\\ &\text{for } N=3,7,11,\dots,\\ &|p_0|=\pi/2(1-1/N)\ ,\ |p_1|=\pi/2(1+3/N)\\ &\text{for } N=9,13,\dots\ . \end{aligned} \tag{2.14}$$

The validity of these rules for odd values of $N\neq5$ can be verified by means of the Bethe ansatz. For $N=5$, the momentum of the ground state is $|p_0|=\pi/2(1-\frac{1}{5})$ in accord with (2.14). The momentum of the first excited state, however, is zero. Conformal invariance[8] gives predictions for the finite-size behavior of the ground state and of the first excited state with periodic boundary conditions

$$\varepsilon_0(N)-\varepsilon_0(\infty)=\pi^2a/(6N^2)\ , \tag{2.15}$$

$$\varepsilon_1(N)-\varepsilon_0(N)=\pi^2b/N^2\ . \tag{2.16}$$

For N even, this behavior has been verified numerically in Ref. 9 and the constants a and b, which can be identified with the central charge, turn out to be one. To our knowledge, predictions of conformal invariance for the finite-size behavior of the lowest states in the AFH model with N odd have not yet been worked out. We observe, in our results for $N=13,15$ and in the previous results of Bonner and Fisher[6] for $N=5,7,9,11$ a behavior of the forms (2.15) and (2.16), but the constants a and b seem to be quite different from the case where N is even:

$$a=-2.04\ ,\quad b=1.83\ . \tag{2.17}$$

It should be noted that the ground-state energies $\epsilon_0(N)$ for N even and N odd approach the thermodynamical limit from below and above, respectively,

$$\epsilon_0(N)|_{N\ \text{even}}<\epsilon_0(\infty)<\epsilon_0(N)|_{N\ \text{odd}}\ . \tag{2.18}$$

Apart from the trivial s_3 degeneracy, we found for the ring with $N=16$ sites the following degeneracies in the spectrum of energy eigenvalues;

(1) For $E\neq2,4,6$ all eigenstates (2.10) and (2.11) with $p\neq0,\pi$ are exactly twofold degenerate. All nondegenerate eigenstates are symmetric under the reflection operator R and have quantum numbers $(p=0,\pi;\ \lambda=0)$.

(2) The eigenstates with energy eigenvalues $E=2,4,6$ show additional degeneracies, which are not related to the reflection symmetry R: (a) There are two eigenstates with $E=2$ and $p=0$:

$$\begin{aligned} &|E=2,s=5,s_3,p=0,\lambda=0\rangle\ ,\\ &|E=2,s=6,s_3,p=0,\lambda=0\rangle\ . \end{aligned} \tag{2.19}$$

Note, that the two states differ in their total spin. (b) There are eight states with $E=4$ and $p=\pi$:

$$\begin{aligned} &|E=4,s=4,s_3,p=\pi,\lambda=0\rangle\ ,\\ &|E=4,s=7,s_3,p=\pi,\lambda=0\rangle\ ,\\ &|E=4,s=6,s_3,p=\pi,\lambda=\pm6.942235\rangle\ ,\\ &|E=4,s=6,s_3,p=\pi,\lambda=\pm12.50881\rangle\ ,\\ &|E=4,s=6,s_3,p=\pi,\lambda=\pm15.59532\rangle\ , \end{aligned} \tag{2.20}$$

(c) There are three states with $E=6$:

TABLE I. The energies per spin and the momenta of the ground state and the first excited state for rings with an odd number of sites.

N	3	5	7	9	11	13	15
$-\varepsilon_0(N)$	0.5	0.747 21	0.815 77	0.843 84	0.857 99	0.866 089 8	0.871 155 6
$p_0N/2\pi$	1	1	2	2	3	3	4
$-\varepsilon_1(N)$	-0.5	0.3	0.516 078	0.696 04	0.725 821 3	0.769 519 3	0.797 573 8
$\|p_1\|N/2\pi$	0	0	1	3	2	4	3

$$\begin{aligned}&|E=6,s=7,s_3,p=\pm\pi/2\rangle\ ,\\&|E=6,s=6,s_3,p=\pi,\lambda=0\rangle\ .\end{aligned}\tag{2.21}$$

Here, the states differ in their total spin $\Delta s=1$ and momenta $\Delta p=\pm\pi/2$. This type of degeneracy can be found on all rings with an even number of sites.

The density of states $N(E,s)$ as a function of the energy E is plotted in Figs. 1(a)–1(f) for the total spin sectors $s=0,1,2,3,4,5$ of a ring with $N=16$ sites. These distributions show some characteristic features: (1) Small energy eigenvalues, which determine the low-temperature behavior, are accompanied by small values of the total spin $s=0,1,2$. (2) The maximum of the distribution $N(E,s)$ and its average value increase with s. The distribution of the nondegenerate eigenvalues, which are all zero modes of F_3, are marked in black.

III. INTERNAL ENERGY AND ENTROPY

From the distribution of the energy eigenvalues, presented in the last section, we obtain the thermodynamical properties of the AFH ring. The internal energy per site

$$U(T,N)/N=\frac{1}{NZ}\sum_E N(E)E\exp(-E/kT)\tag{3.1}$$

and the entropy per site

$$S(T,N)/N=\frac{1}{TN}[U(T,N)-F(T,N)]\ ,\tag{3.2}$$

where $F(T,N)$ and $Z(T,N)$ are the free energy and the partition function, respectively,

$$F(T,N)=-kT\ln Z(T,N)\ ,\tag{3.3}$$

$$Z(T,N)=\sum_E N(E)\exp(-E/kT)\ ,\tag{3.4}$$

$$N(E)=\sum_s(2s+1)N(E,s)\ ,\tag{3.5}$$

are shown in Figs. 2 and 3 together with the results for $N=11$ of Ref. 6. It has been already observed by Bonner and Fisher[6] that the internal energy per site $u(T)$ and the entropy per site $s(T)$ in the thermodynamical limit $(N\to\infty)$ are bounded from below and above by the corresponding quantities on finite systems with N even and odd, respectively,

$$U(T,N)/N|_{N\text{ even}}<u(T)<U(T,N)/N|_{N\text{ odd}}\ ,\tag{3.6}$$

$$S(T,N)/N|_{N\text{ even}}<s(T)<S(T,N)/N|_{N\text{ odd}}\ .\tag{3.7}$$

The upper and lower bounds coincide for T values:

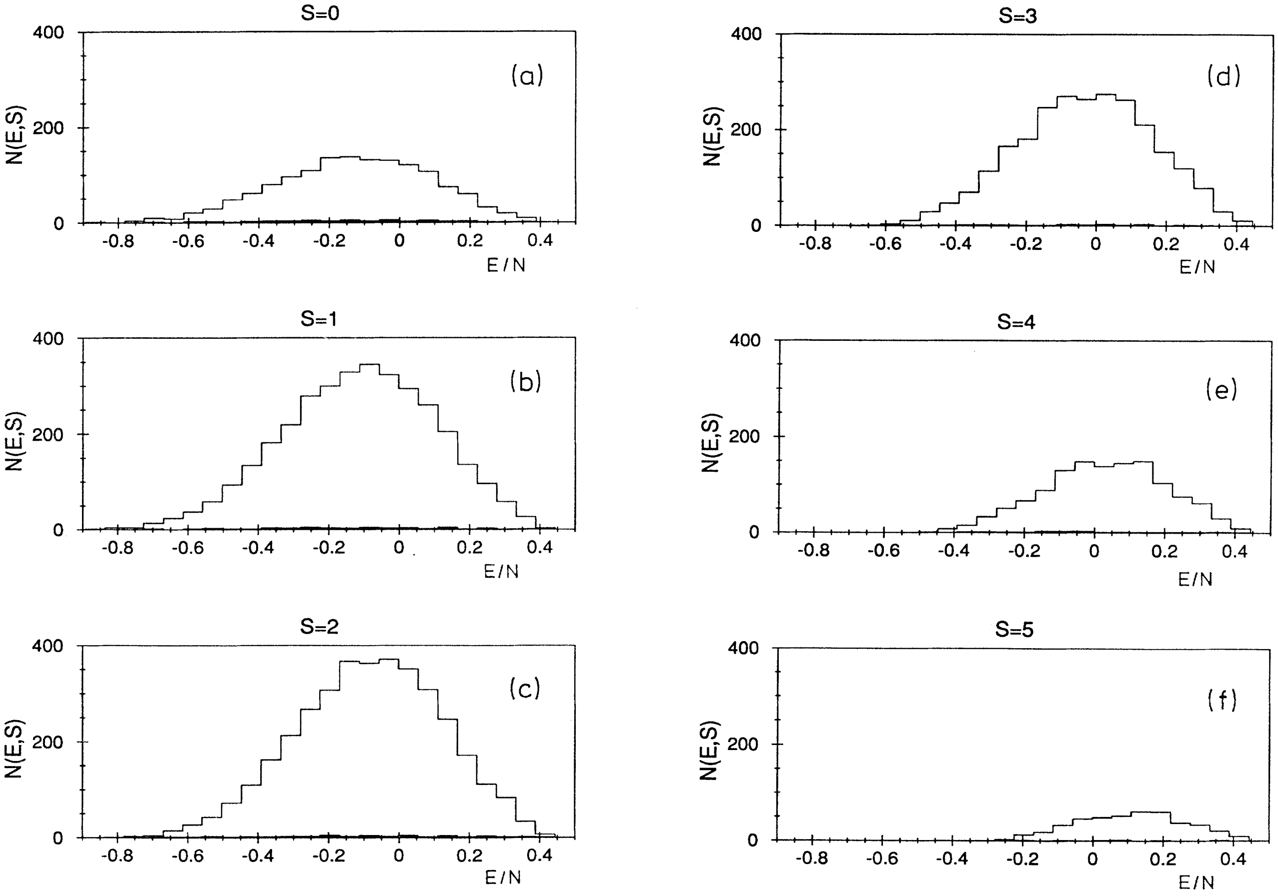

FIG. 1. The densities of states $N(E,s)$ in the sectors with total spin $s=0$, 1, 2, 3, 4, and 5 on a ring with $N=16$ sites.

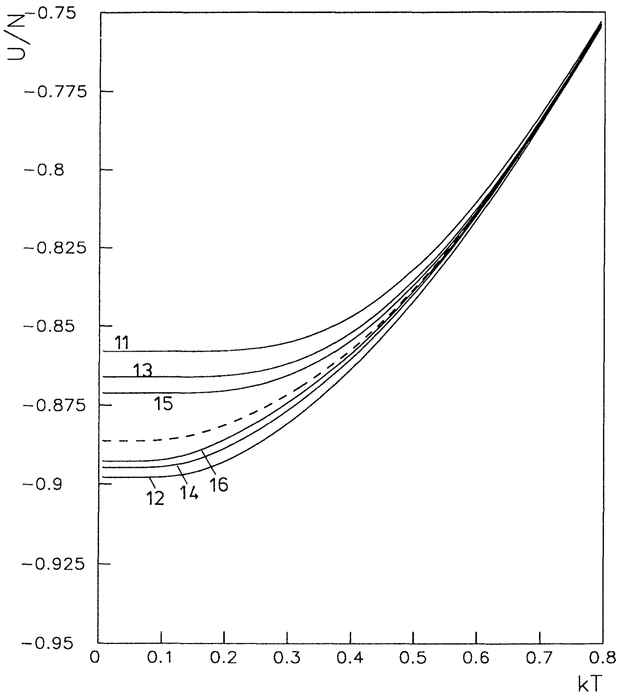

FIG. 2. The internal energy per site vs temperature.

$$kT > 08 \ . \tag{3.8}$$

In this domain we see already on finite systems ($N > 10$) the limiting behavior for $N \to \infty$. This is not so in the low-temperature domain, where we feel the finiteness of the system. This indicates already that the correlation length is increasing as we approach zero temperature. The correlation length will be investigated in Sec. V. One might ask whether the bounds (3.6) and (3.7) may help to find a clever extrapolation to the thermodynamical limit. For example, Bonner and Fisher introduced weighted means of their results for $N = 10$ and 11 in order to estimate the low-temperature behavior in the thermodynamical limit.

Here, we propose weighted means of our results for $N = 15$ and 16:

$$\begin{aligned} \bar{u}(T) &= p(15)U(T,15)/15 + p(16)U(T,16)/16 \ , \\ \bar{s}(T) &= p(15)S(T,15)/15 + p(16)S(T,16)/16 \ . \end{aligned} \tag{3.9}$$

We will assume that the weights $p(15)$ and $p(16)$ are independent of the temperature and are the same for all observables. Since we know the ground-state energy per site in the infinite system from the Bethe ansatz,

$$u(T=0) = \tfrac{1}{2} - 2\ln 2 \ , \tag{3.10}$$

we can compute the weights

$$p(15) = 0.300\,35 \ , \quad p(16) = 0.699\,65 \ . \tag{3.11}$$

The weighted means (3.9) are represented in Figs. 2 and 3 by dashed curves. The thermodynamical Bethe ansatz[10] and conformal invariance[11] predict a linear behavior at low temperatures for the specific heat and the entropy per site in the thermodynamical limit

$$C = 1/3kT \ , \tag{3.12}$$

$$S/Nk = 1/3kT \ , \tag{3.13}$$

with slope $\frac{1}{3}$. This behavior is represented in Fig. 3 as a straight line which is almost tangent to our extrapolation (3.9) with the weights (3.11).

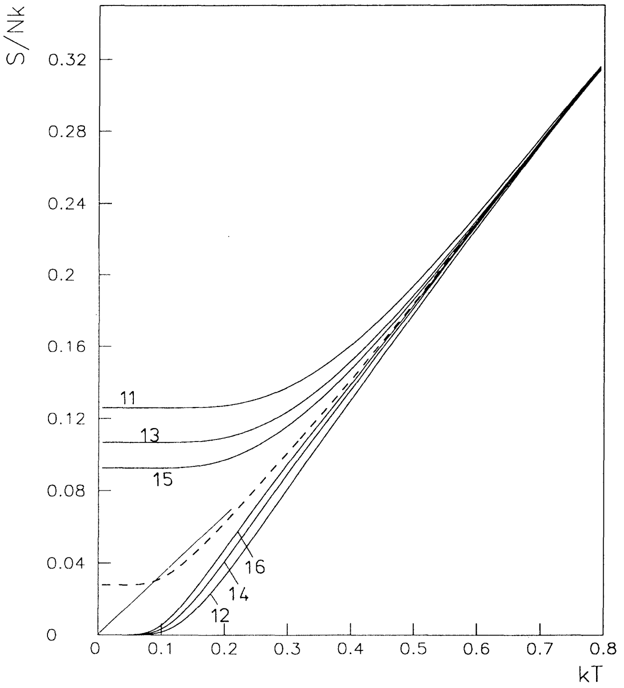

FIG. 3. The entropy per site vs temperature. The straight line shows the low-temperature behavior (3.12).

IV. MAGNETIC PROPERTIES AND TOTAL SPIN AVERAGES

In the absence of an external field, the susceptibility per spin

$$\chi(T,N) = \frac{1}{kT}\Xi(T,N) \tag{4.1}$$

can be expressed in terms of the thermal average of the operator $\mathbf{S}^2$:

$$\begin{aligned} \Xi(T,N) &= (1/N)\left\langle \left[\sum_x S_3(x)\right]^2 \right\rangle(T) \\ &= (1/3N)\langle \mathbf{S}^2 \rangle(T) \\ &= (1/3N)\sum_s s(s+1)Z(T,s) \Big/ \sum_s Z(T,s) \ . \end{aligned} \tag{4.2}$$

Here we denote by

$$Z(T,s) = (2s+1)\sum_E N(E,s)\exp(-E/kT) \tag{4.3}$$

the partition function in the spin-s sector. Since we know the distributions $N(E,s)$ of energy eigenvalues in the various spin sectors, the computation of the susceptibility is straightforward. For a study of the thermodynamical limit $N \to \infty$, the quantity $\Xi(T,N)$ appears to be more useful than the susceptibility itself. We expect that the sequence $\Xi(T,N)$ has a proper limit for $N \to \infty$:

$$\lim_{N \to \infty} \Xi(T,N) = \Xi(T) \tag{4.4}$$

and that the limiting function $\Xi(T)$ behaves as

$$\Xi(T) = \begin{cases} \text{const} & \text{for } T \to \infty \ , \\ \chi(0) kT & \text{for } T \to 0 \ . \end{cases} \tag{4.5}$$

The high-temperature behavior expresses Curie's law, whereas the low-temperature behavior means that the susceptibility per spin converges to a finite nonvanishing value. According to Griffiths conjecture,[12] the susceptibility at $T=0$ is $\chi(0)=0.050\,66$.

The $\Xi(T,N)$ with N even (odd) approach, the limiting curve (4.4) from below (above):

$$\Xi(T,N)|_{N,\text{even}} < \Xi(T) < \Xi(T,N)|_{N,\text{odd}} \ . \tag{4.6}$$

This behavior is easily understood in the low-temperature limit: For $N=3,5,\ldots$, the total spin values are half-integers $s=\frac{1}{2},\frac{3}{2},\ldots$. The (antiferromagnetic) ground state is found in the spin $s=\frac{1}{2}$ sector. Therefore, we expect

$$\Xi(T,N) \sim 1/(4N) \quad \text{for } T \to 0, \quad N=3,5,\ldots \ . \tag{4.7}$$

For $N=4,6,\ldots$, the total spin values are integers $s=0,1,2,\ldots$. The ground state is found in the $s=0$ sector the first excited state in the $s=1$ sector,

$$\Xi(T,N) \sim (2/N)\exp(-\Delta E/kT) \ , \tag{4.8}$$

where ΔE is the gap between the ground state and the first excited state.

The temperature dependence of $\Xi(T,N)$ for $N=11,13,15$ and $N=12,14,16$ is shown in Fig. 4. The dashed curve again represents the weighted mean

$$\overline{\Xi(T)} = p(15)\Xi(T,15) + p(16)\Xi(T,16) \tag{4.9}$$

with weights (3.11). The linear low-temperature behavior (4.5) (with the slope given by the Griffiths value) is almost tangent to our extrapolation. This supports our assumption (3.11) on the weights in Eq. (4.9).

V. SPIN-SPIN CORRELATION FUNCTIONS AND THE CORRELATION LENGTH

In the absence of an external field, the spin-spin correlation functions are defined as

$$\begin{aligned} \omega_l(N) &= 4\langle S_3(x) S_3(x+l) \rangle \\ &= \tfrac{4}{3} Z^{-1} \text{Tr}[\exp(-H/kT) \mathbf{S}(x) \cdot \mathbf{S}(x+l)] \ . \end{aligned} \tag{5.1}$$

The correlation functions multiplied with a factor $(-1)^l$ are shown for $N=15$ and 16 in Figs. 5 and 6 as function of the separation l and the temperatures

$$kT = 0.2, 0.4, 0.6, 0.8, 1.0, 2.0, 3.0, 4.0, 5.0, 6.0 \ .$$

For even N, the data points are well described by a

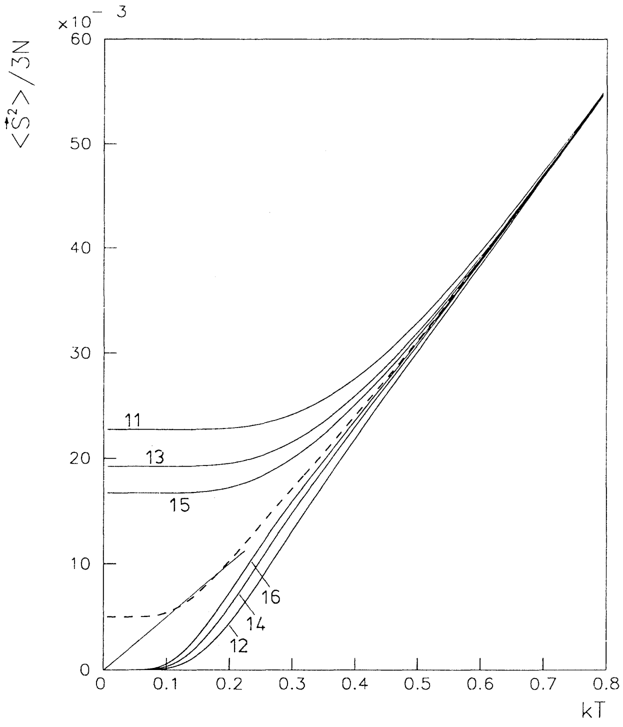

FIG. 4. The thermal average of $\mathbf{S}^2$ vs temperature. The straight line shows the low-temperature behavior (4.5) with the Griffiths value for the susceptibility $\chi(0)=0.050\,66$.

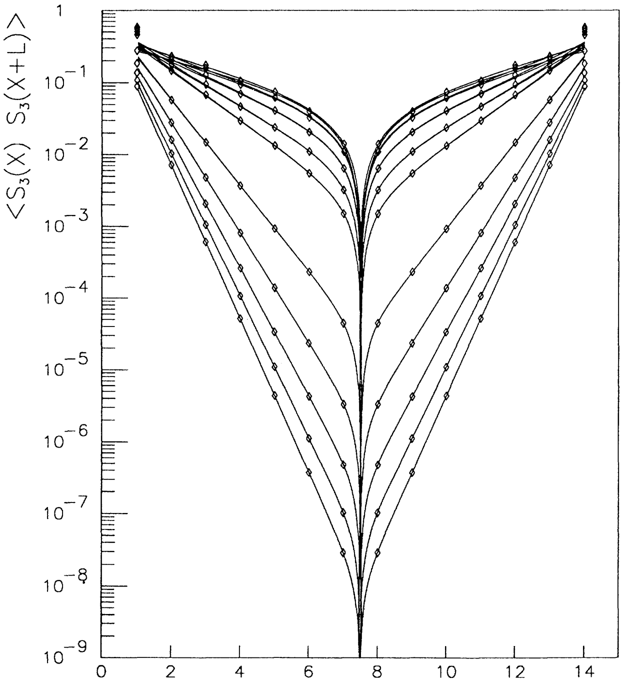

FIG. 5. The spin-spin correlators as a function of the separation l for $N=15$. The solid lines are extrapolations according to Eq. (5.4).

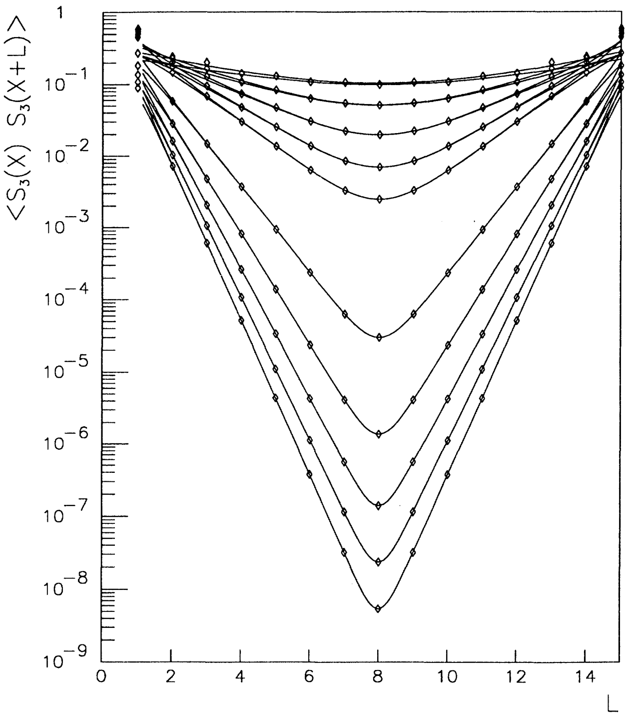

FIG. 6. Same as in Fig. 5 for $N=16$. The solid lines are extrapolations according to Eq. (5.3).

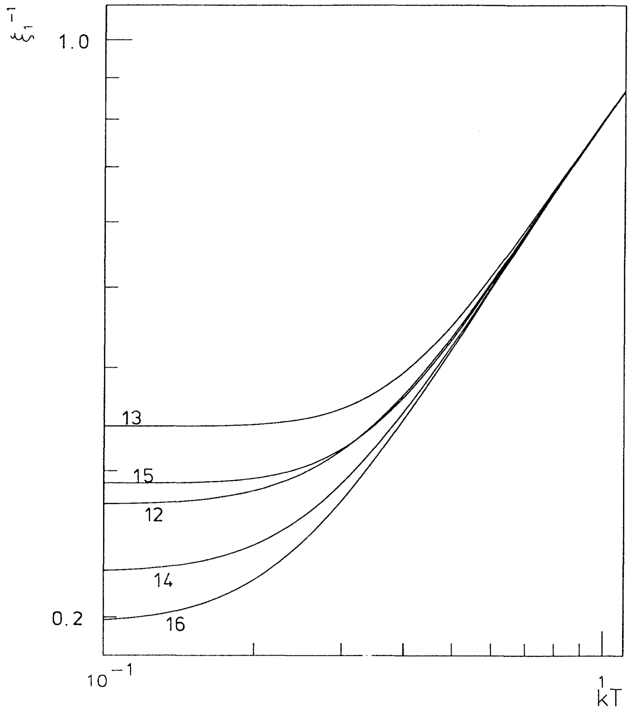

FIG. 7. The inverse correlation length $[\xi_1(T,N)]^{-1}$ vs temperature.

hyperbolic-cosine-type ansatz,

$$\omega_l(N)=(-1)^l A_l(T,N)\cosh[(N/2-l)/\xi_1(T,N)] + A_2(T,N)\cosh[(N/2-l)/\xi_2(T,N) \ , \qquad (5.2)$$

whereas one observed a mixed behavior for odd N,

$$\omega_l(N)=(-1)^l A_1(T,N)\sinh[(N/2-l)/\xi_1(T,N)] + A_2(T,N)\cosh[(N/2-l)/\xi_2(T,N)] \ . \qquad (5.3)$$

Note that all the terms in (5.2) and (5.3) respect the symmetry property of the correlation functions

$$\omega_l(N)=\omega_{N-l}(N) \ . \qquad (5.4)$$

The amplitudes $A_i(T,N)$, $i=1,2$, and the correlation lengths $\xi_i(T,N)$, $i=1,2$, were determined from the correlators at the four innermost sites. For an unambiguous determination of these parameters, it is crucial that our correlation functions are calculated exactly. In general, the mere existence of statistical errors in a Monte Carlo simulation prevents a clean separation of the lowest mode (with correlation length ξ_1) from the excited modes.

The inverse correlation length $\xi_1^{-1}(T,N)$ as a function of the temperature and the number of sites $N=12$, 13, 14, 15, and 16 is shown in Fig. 7 in a log-log-plot. The curves coincide for temperatures $kT>0.8$ and split below this value due to finite-size effects. There are strong arguments that the system becomes critical at $T=0$ in the thermodynamical limit.[13] Therefore, we expect the correlation length $\xi_1(T,N)\rightarrow\infty)$ to diverge at $T=0$. In this case, a standard finite-size scaling ansatz[14] should be applicable:

$$\xi_1(T,N)/\xi_1(T,N\rightarrow\infty)=f[N/\xi_1(T,N\rightarrow\infty)] \ . \qquad (5.5)$$

To our knowledge, the type of the divergence in the correlation length is not known so far for the one-dimensional AFH model. It may be an exponential one—as it appears to be in the two-dimensional case[15]—or an algebraic one. We tried to answer this question by analyzing our data with the scaling ansatz (5.5). We found that an exponential singularity does not fit, whereas the power-law ansatz

$$\xi_1(T,N\rightarrow\infty)\sim(kT)^{-\nu} \qquad (5.6)$$

leads to good results for ν values close to one. Figures 8 and 9 show the scaling functions (5.5) for $\nu=1.0$, $N=12,14,16$ and $N=13,15$, respectively. The rescaled correlation lengths coincide almost exactly near the phase-transition point $T=0$. However, the scaling functions differ slightly from each other for the N-even and N-odd cases. This is an accord with our experience of other thermodynamical quantities: The approach to the thermodynamical limit is quite different for N even and N odd. If one changes the critical exponent ν, the scaling behavior starts to disappear at $\nu<0.95$ and $\nu>1.05$. This gives an estimate on the error in ν. The subleading correlation lengths ξ_2 are plotted in Fig. 10 for $N=12$, 13, 14, 15, and 16. They seem to suffer much more under finite-size effects. Concerning the amplitudes $A_i(T,N)$,

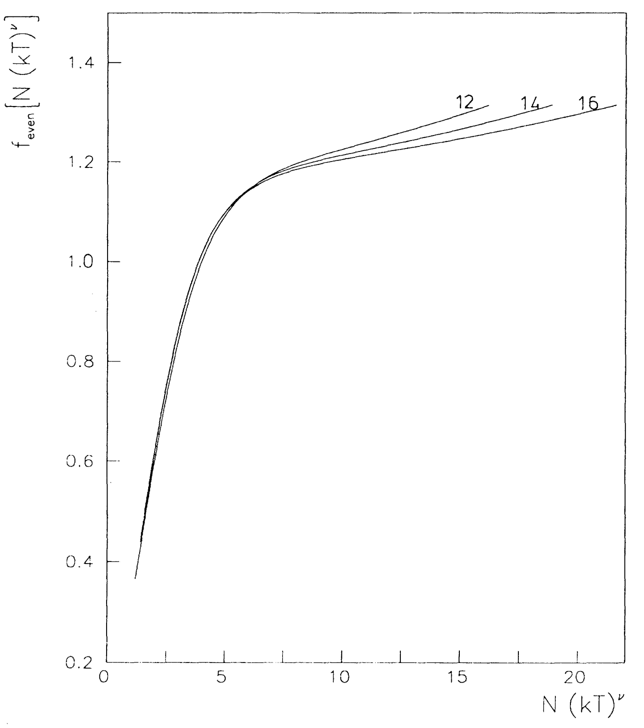

FIG. 8. The scaling function (5.6) for $\nu=1.0$ and $N=12$, 14, 16.

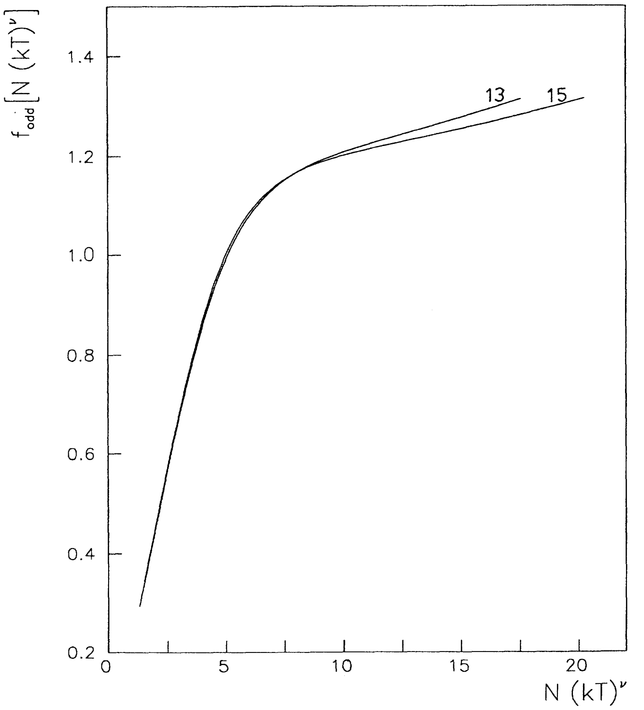

FIG. 9. Same as Fig. 8 for $N=13,15$.

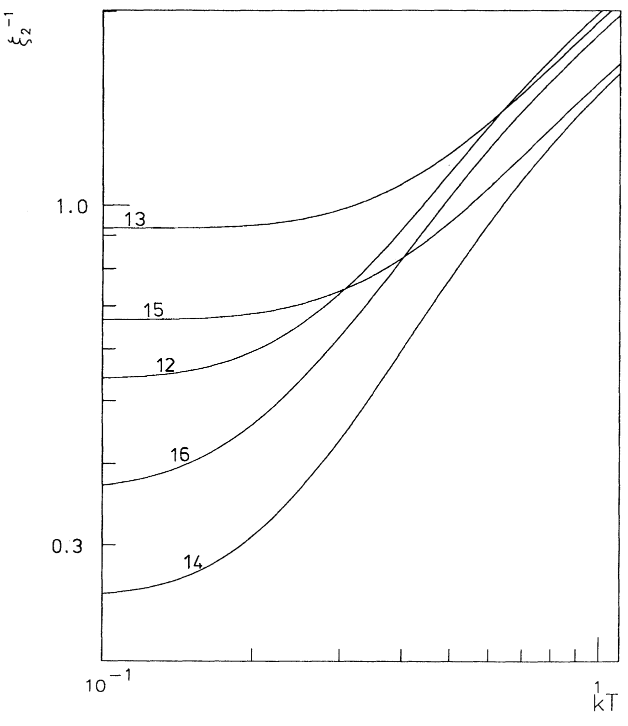

FIG. 10. The inverse correlation length $[\xi_2(T,N)]^{-1}$ vs temperature.

$i=1,2$, in our parametrizations (5.2) and (5.3), we only want to mention that they are stable in the following sense: $A_1(T,N)$ shows the T dependence, as we expect it from $\omega_0(N)=1$; $A_2(T,N)$, which is much smaller than $A_1(T,N)$, decreases for increasing T values.

Finally, it should be noted, that the parametrizations (5.2) and (5.3) are applicable for nonvanishing temperatures only. At $T=0$, the correlation functions are known[13] to decrease as $(-1)^l/l$ for large separations l. For our finite values of N and T, we were not able to disentangle the subleading power-law behavior from the leading exponential behavior. Indeed, looking for an optimal parametrization, we realized that the subleading contributions to the correlators are best fitted by a second exponential.

VI. THERMAL AVERAGE OF A HIGHER CONSERVATION LAW

Having classified the energy eigenstates (2.10) by the quantum numbers H, $\mathbf{S}^2$, S_3, P, and F_3, it is straightforward to compute the thermal averages of any function $f(E,s,s_3,p,\lambda)$. The results for the internal energy and the thermal average of $\mathbf{S}^2$ with N even and N odd seem to indicate that they yield lower and upper bounds for the behavior of these quantities in the thermodynamical limit. This motivated us to look whether bounds of the type (3.6) and (4.6) also exist for the thermal average of the operator F_3^2:

$$f_3(T,N)|_{N\ \mathrm{even}}<f_3(T)<f_3(T,N)|_{N\ \mathrm{odd}} \qquad (6.1)$$

where

$$f_3(T,N)=(1/N)\langle F_3^2\rangle(T,N)\ . \tag{6.2}$$

Indeed, this behavior is clearly seen in Fig. 11 where we have plotted the thermal averages for $N=13,15$ and $N=14,16$, respectively.

VII. THERMAL AVERAGE OF THE MOMENTUM

In Sec. II we pointed out that the modulus of the momentum in the ground state converges to three different values $|p|=0,\pi/2,\pi$, depending on how we approach the thermodynamical limit: $N=2(n+1),n,2n$, where n is an odd number going to infinity. This peculiar feature is shown in Fig. 12, where we have plotted the thermal average $\langle |p|\rangle(T,N)$ as a function of the temperature T and the number of sites $N=13$, 14, 15, and 16. For these finite values of N, the thermal averages differ in the low-temperature interval $kT<0.5$, but coincide above this value:

$$\langle |p|\rangle(T,N)=\pi/2$$
$$\text{for } T>0.8 \text{ and } N=13,14,15,16\ . \tag{7.1}$$

We suggest that the splitting of $\langle |p|\rangle(T,N)$ at nonzero temperatures $T\neq 0$ is a finite-size effect. Indeed, in all the observables we investigated so far, finite-size dependences were visible on our systems at $kT<0.8$. Therefore, we expect that, in the thermodynamical limit,

$$\langle |p|\rangle(T,N\rightarrow\infty)=\pi/2 \ \text{ for } T>0\ . \tag{7.2}$$

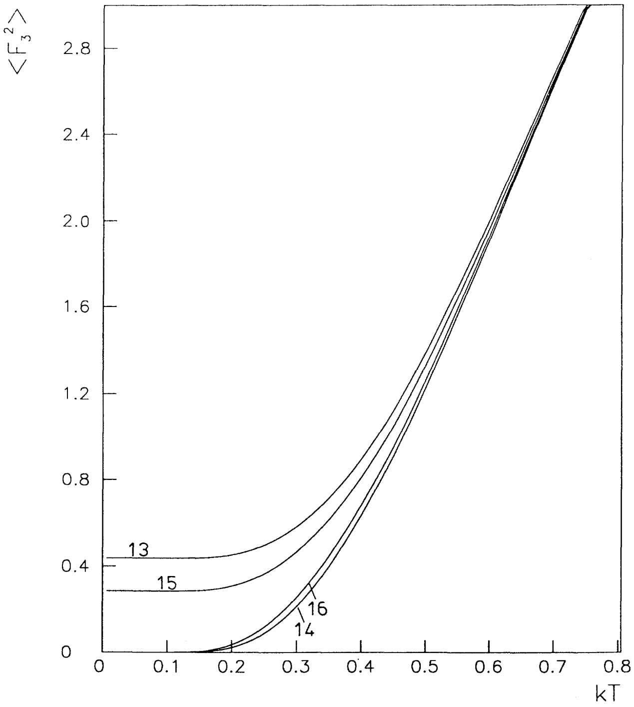

FIG. 11. The thermal average of the conserved operator F_3^2.

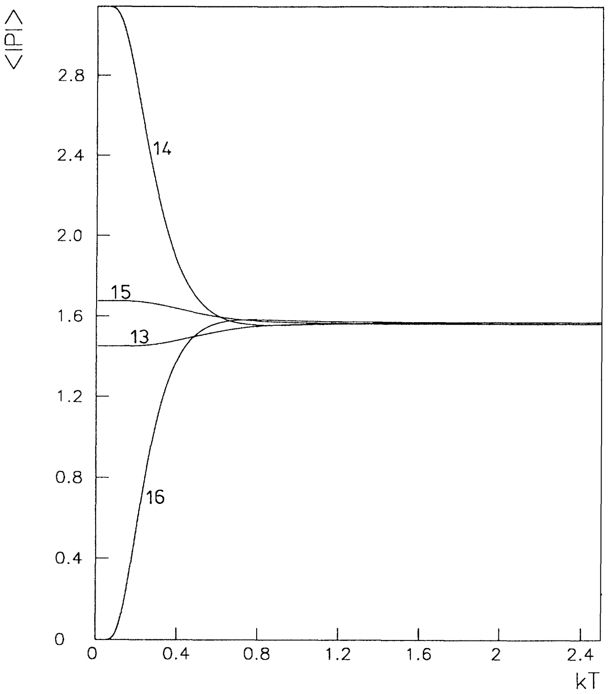

FIG. 12. The thermal average of the modulus of the momentum.

At first sight this behavior appears to be unusual. For example, in a free Boltzman gas, the thermal average $\langle |p|\rangle(T)$ is proportional to $\sqrt{T}$, due to the dispersion relation between energy and momentum. In a quantum system— with N momenta $p=2\pi n/N$, $n=0$, $\pm 1,\pm 2,\ldots$ and 2^N energy eigenvalues—the notion of a dispersion relation is not obvious. Since the momentum is a conserved quantity, it is reasonable to split the Hilbert space of energy eigenstates into sectors of definite momentum p. The most simple "explanation" of the behavior (7.2) would be that the distribution of the energy eigenvalues $N(E,p)$ in the different sectors is the same for all momenta p (in the thermodynamical limit). The distributions $N(E,p)$ plotted in Figs. 13(a)–13(i) for a ring with 16 sites indicate that such a hypothesis might be correct.

A behavior of the type (7.2) is quite plausible in the Ising model. The distributions of the eigenvalues of the Ising-Hamiltonian—which is obtained from (2.1) by the substitution $\sigma(x)\cdot\sigma(x+1)\rightarrow\sigma_3(x)\sigma_3(x+1)$—are "almost" momentum independent, since two spin configurations which are related by a translation have the same energy eigenvalue. In general, this implies that the energy eigenvalues are momentum degenerate. However, this does not hold for spin configurations with special symmetries under translations, which only allow for special p values. For example, the configuration with all spins parallel has momentum 0 only.

In this context, it is worthwhile to note how the antiferromagnetic ground-state properties of the classical Ising Hamiltonian differ from those in the quantum Heisenberg model: For N even, the ground state of the Ising Hamiltonian is twofold degenerate; there are two possibilities to construct Néel states with complete antiferromagnetic ordering. If the momentum operator is diagonalized, the momentum eigenvalues turn out to be 0 and π.

For N odd, the ground state of the Ising Hamiltonian

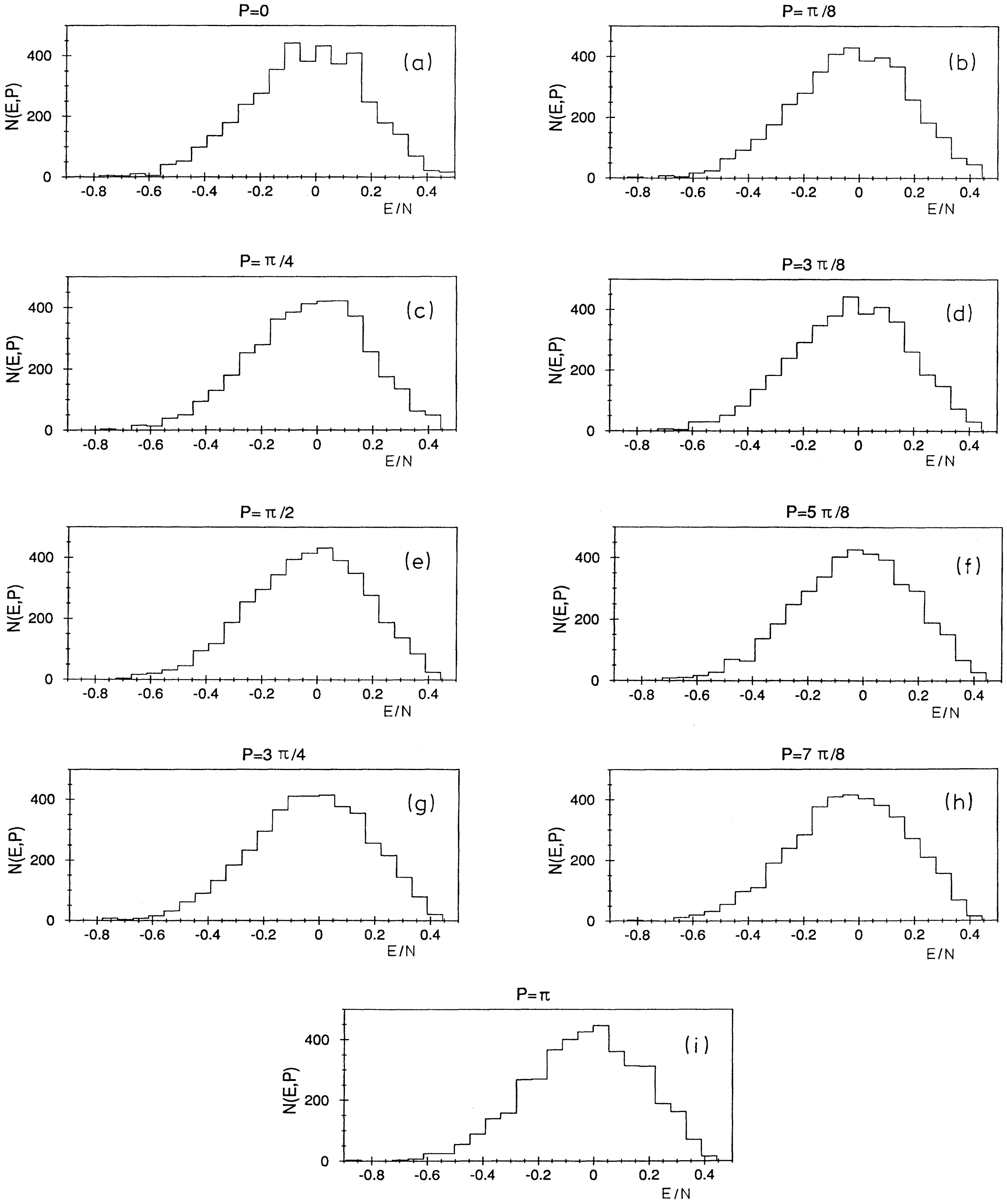

FIG. 13. The densities of states $N(E,p)$ in the sectors with momentum p on a ring with $N=16$ sites.

is $2N$ −fold degenerate. This is the number of states with only one pair of parallel spins. If the momentum operator is diagonalized, each momentum value is found twice.

Therefore, the thermal average $\langle |p| \rangle (T,N)$ will be equal to $\pi/2$ for all values of T in the Ising system. In particular, there will be no splitting, as we observed it in the AFH model for finite N.

VIII. CONCLUSIONS

By means of an exact and complete diagonalization of the AFH Hamiltonian for rings with

$$N = 11, 13, 15,$$

and

$$N = 12, 14, 16$$

sites, we have determined the following quantities $q(T,N)$ as function of the temperature T and the number of sites: internal energy per site, $U(T,N)/N$; entropy per site, $S(T,N)/N$; thermal average, $\langle \mathbf{S}^2 \rangle (T,N)/3N$; and thermal average of the conserved operator (2.7), $\langle F_3^2 \rangle (T,N)/N$. Combining our results with those of Ref. 6, we come to the following conclusion: For all values of the temperature T, the quantities $q(T,N)$ decrease monotonically for $N=3$, 5, 7, 9, 11, 13, and 15 and increase monotonically for $N=4$, 6, 8, 10, 12, 14, and 16. This is, of course, a strong indication that the $q(T,N)$ on finite systems with N odd and N even yield monotonic upper and lower bounds on these quantities in the thermodynamical limit

$$q(T,N)|_{N \text{ even}} < q(T,N \to \infty) < q(T,N)|_{N \text{ odd}} .$$

To our knowledge, there does not yet exist a rigorous proof for these bounds. Our results on the thermal spin-spin correlation functions yield strong evidence for a diverging correlation length $\xi(T,N\to\infty) \sim T^{-1}$ if we approach the critical point $T \to 0$.

From our computations of the thermal average $\langle |p| \rangle (T)$, we conclude that this quantity is exactly $\pi/2$ in the thermodynamical limit for all temperatures $T>0$. The origin of such a behavior has to be sought in the nontrivial dynamics of the one-dimensional quantum Heisenberg system with its infinite series of higher conservation laws. It will be interesting to see whether a similar behavior can be found in the two-dimensional cases as well.

The fact that the momentum of the ground state is $\pi/2$ and π if we approach the thermodynamical limit with $N=n$ and $2n$, n odd, can be interpreted as a spontaneous symmetry breaking of translation invariance: In contrast to the Hamiltonian, the ground state is not invariant under all translations. More precisely, the ground state is not changed by translations, which are multiples of 4 for $N=n$ and of 2 for $N=2n$.

ACKNOWLEDGMENTS

We thank S. Dietrich and R. Sommer for a discussion on the "best" parametrizations of spin-spin correlators and G. v. Gehlen for informing us on recent results on conformal invariance of quantum spin chains. M. Karbach verified Eq. (2.14) by means of the Bethe ansatz.

---

[1] H. A. Bethe, Z. Phys. **71**, 205 (1931); L. Hulthén, Arkiv Mat. Astron. Fys. **26A**, 1 (1938).

[2] M. Lüscher, Nucl. Phys. **B117**, 475 (1976).

[3] K. Fabricius, K.-H. Mütter, and H. Grosse, Phys. Rev. B **42**, 4656 (1990).

[4] J. Oitmaa and D. D. Betts, Can. J. Phys. **56**, 897 (1978); J. Borysowicz, P. Horsch, and T. Kaplan, Phys. Rev. B **31**, 1590 (1985).

[5] E. Dagatto and A. Moreo, Phys. Rev. B **38**, 5087 (1989).

[6] J. C. Bonner and M. E. Fisher, Phys. Rev. **135**, A640 (1964).

[7] J. E. Hirsch, R. L. Sugar, D. J. Scalapino, and R. Blankenbecler, Phys. Rev. B **26**, 5033 (1982).

[8] J. L. Cardy, in *Phase Transitions and Critical Phenomena*, edited by C. Domb and J. L. Lebowitz (Academic, London, 1987), Vol. 11.

[9] C. J. Hamer, J. Phys. A **18**, L1133 (1985); **19**, 3336 (1986); H. P. Eckle, Ph.D. Dissertation, Freie Universität Berlin, 1989.

[10] H. M. Babujian, Nucl. Phys. **B215**, 317 (1982).

[11] I. Affleck, Phys. Rev. Lett. **56**, 746 (1986).

[12] R. G. Griffiths, Phys. Rev. **133**, A768 (1964); C. N. Yang and C. P. Yang, *ibid.* **151**, 238 (1966).

[13] A. Luther and I. Peschel, Phys. Rev. **135**, A640 (1964); A. G. Izergin and V. E. Korepin, Pis'ma Zh. Eksp. Teor. Fiz. **42**, 414 (1985) [JETP Lett. **42**, 512 (1985)].

[14] M. E. Fisher, in *Proceedings of the International School of Physics* "Enrico Fermi," Course 51, Varenna, 1990, edited by M. S. Green (Academic, New York, 1971), p. 1.

[15] H. Q. Ding and M. S. Makivić, Phys. Rev. Lett. **64**, 1449 (1990); Phys. Rev. B **43**, 3562 (1991).